
Article:
Leong, Z., Morley, N. orcid.org/0000-0002-7284-7978 and Goodall, R. orcid.org/0000-0003-0720-9694 (2021) Dilatational strain biplots against enthalpy of mixing for predicting high-entropy alloys and complex concentrated alloys phase stability. Materials Chemistry and Physics, 262. 124241. ISSN 0254-0584

https://doi.org/10.1016/j.matchemphys.2021.124241

Dilatational strain biplots against enthalpy of mixing for predicting high-entropy alloys and complex concentrated alloys phase stability

LEONG Zhaoyuan*, Nicola MORLEY, and Russell GOODALL

*Corresponding author

Department of Materials Science and Engineering, University of Sheffield

Abstract

Multiple principle component alloy systems are a new class of alloys that can provide interesting combinations of functional and mechanical properties. Due to the multiple principle components, their interactions are complex, and their structural stabilities are often not easily predicted. Prediction parameter biplots offer a good way to distinguish between structural stabilities of different compositions. The enthalpy of mixing is one parameter that is often used in such biplots. Although it does not accurately follow quantum principles, it is nevertheless this deviation that gives it its predictive power when combined with other parameters in a biplot. This deviation can be in part attributed to the mechanical strain energy (from large atomic size difference) that may be present in alloy systems. Such a biplot can leverage on their expected deviations to provide a prediction scheme. Here, we investigate the predictive efficacy of enthalpy-of-mixing/strain-energy biplots using cluster analysis. The results are validated against enthalpy-of-mixing/valence electron concentration biplots. The investigated biplot not only maintains the ability to distinguish between the intermetallic and solid solutions phases but offers enhanced ability to distinguish between individual intermetallic phases (Sigma, Laves, Mu, and B2).

Keywords CCA; HEA; Classification; Cluster analysis; Alloy design

1. Introduction

The history of metallurgy is a significant part of human history, and most of its principles are well established. The discovery of multiple component alloy systems [1,2] is a new in the field. These alloy systems may remain in a near-ideal solid solution (these are known as High-entropy alloys, HEAs), or in multi-phased systems, known as Complex Concentrated Alloys, CCAs [3]. These alloy systems are characterised by the high number of alloying components (typically >4) in near-equal molar concentrations (5-30 at.%).

The prediction of stabilities of multiple-component alloy systems is required, as both CCAs and HEAs possess interesting properties that can be leveraged for different uses. For very time-efficient calculations, a combination of the Hume-Rothery rules and thermodynamic parameters may be used with reasonable accuracy. Models based on the classic Hume-Rothery rules and thermodynamic parameters were initially developed for pure and dilute metallic systems, though they tend to have some deviations from experimental results [4–9]. Other models have also been developed for more accurate predictive purposes [10–14].

Increased accuracy for the classic rules may be obtained by using data analysis methods to explore the variations in the important parameters, and reduce these to variables which can be shown graphically in biplots. Dominguez *et al.* [15] demonstrated and validated this through the use of principal component analysis: in this work a biplot of the enthalpy of mixing, ΔH and valence electron concentration, VEC was found to predict HEA/CCA stabilities with increased accuracy, which was further improved if the rule-of-mixture, ROM valence electron concentration parameter was replaced with ROM electronegativity values. Ye *et al.* [16] reported on the importance of shear strain in MCAs. The elastic-strain energy parameter, ΔH_{El} was investigated by Andreoli *et al.* [10] in a biplot against the atomic size difference, the

enthalpy of mixing, and valence electron concentration. They found that a biplot of the elastic-strain energy parameter against the VEC would lead to better accuracy in predicting HEA formation.

The origin of the VEC-ΔH biplot's ability to discriminate between CCAs and HEAs lies in the deviation of the Miedema ΔH from quantum principles [17], where the ΔH-VEC ratio deviates between 4 < VEC < 7 [5]. This zone is regarded as the area for complex phase (or intermetallic) formation [3,5,15,18]; these are compounds with increased directional bonding and hence less metallic character, and this can provide phenomenological evidence of the deviation. In the quasi-chemical theory used in classical metallurgy [19] deviations where larger heats of mixing occur due to large atomic size differences are attributed to the strain energy.

Our hypothesis is that the partial excess free energy of mixing due to strain energy contribution leads to the thermodynamic deviations, and that this can also be used to as a prediction methodology since the source of these errors is the formation of the intermetallic compounds. In a previous study [5] we analysed the efficacy of ROM electronegativities (Pauling, Allen and Mulliken) *vs.* the enthalpy of mixing, ΔH biplots through cluster analysis and probability distribution functions. This strategy will be employed in this letter to determine the efficacy of the strain energy in biplots against the enthalpy of mixing and to test the hypothesis presented.

2. Theory

Following Miedema's model [20] which is the basis for the majority of the ΔH values used in HEA literature, the basic equation for a binary compound is:

$$\Delta H_{mc} = c_m\, c_c\, (-P\, e\, (\Delta\varphi)^2 + Q(\Delta n_{ws})^2) \qquad \text{(Eq. 1)}$$

here P and Q are empirical constants, c_m and c_c are the concentrations of the metals m and c, e is the elementary charge, $\Delta\varphi$ is the change in chemical potential of the resultant mc alloy, and Δn_{ws} is the change in electron density at the Wigner-Seitz radius. Miedema argued that Δn_{ws} is proportional to the bulk modulus to molar volume ratio, and that $\Delta\varphi$ can be correlated to both the Pauling electronegativity and atomic radius [20]. Δn_{ws} and $\Delta\varphi$ possess radius components (analogous to the atomic size difference parameter), and it is known that adherence to Vegard's law is the exception and not the norm. The analysis of this equation supports our hypothesis; furthermore ΔH and δ biplots [21] also show correlation with the formation of HEA phases, likely due to the deviation from Vegard's law for CCA compounds. The equation can be modified for many component systems using the sub-regular solution model by evaluating each pair interaction [22,23].

Alloying elements (interstitial or substitutional) in solid solution can therefore affect the enthalpy of mixing. The accuracy to which this can be assessed is dependent on the derivation of the enthalpy of mixing model and the selection of its radius components. A comparison between enthalpy of mixing values with calculated dilatational strain values may allow increased accuracy as other contributing factors are not included (*e.g.* the contribution of the valence electrons to elastic parameters is not straightforward, being dependent on other factors such as shielding, spin-orbit coupling *etc.*). To facilitate the comparison, a methodology for calculating the elastic energy must be determined.

Andreoli *et al.* used an elastic-strain energy criterion to demonstrate a design strategy for complex concentrated alloys utilising the following equation [10,13]:

$$\phi_{el} = \sum_{i=1}^{N} \frac{c_i K_i}{2} \frac{(V_i - V)^2}{V_i} \qquad \text{(Eq. 2)}$$

where c_i, K_i, and V_i are the concentration, bulk modulus, and volume of the i^{th} element respectively. V is the average volume of alloying additions weighted by their stoichiometry. The equation is a modified form of the elastic energy of an inclusion in a solid solution under a uniform hydrostatic pressure [24]; but does not consider the contribution to the elastic energy from the matrix, from which arises the $\frac{2\,G_m}{3K_c+4G_m}$ term in Eq. 3. The pairwise interactions between the alloying elements are not included in this formulation, taking the ROM approach to give a reasonable approximation of the total energy. Therefore, in order to increase its accuracy, we modify the equation to account for the shear modulus contribution and pairwise interactions.

For simplicity, the atomic displacements in *A-B* mixtures are taken to behave in a linear elastic manner. The total of the A-B strain energy contributions of a particular composition determined in this way is used to approximate the dilatational strain. The accuracy of the approximation can be improved by application of elastic theory by accounting for the influence of the shear modulus. The equilibrium final radius is obtained by correcting the usual radius used (*i.e.* here, metallic radius of an element). The strain energy is estimated through this determination of the strain energy *per* atom; in the unstrained matrix this is [19,25]:

$$\phi_{dil} = \frac{2\,G_m\,K_c}{3K_c+4G_m} \times \frac{(V_m-V_c)^2}{V_c} \qquad \text{(Eq. 3)}$$

where V_m and V_c are the volumes per molecule for the matrix and the cluster respectively, $E_{Y,m}$ and $E_{Y,c}$ are the Young's modulus for the matrix and the cluster respectively, and v_m and v_c are the Poisson's ratio for the matrix and the cluster respectively. It is possible to use the Voigt average [26], (assuming that a homogenous strain is present in the structure) for cubic structures so that the elastic strain energy, ϕ_{strain} can be expressed as a function of the elastic constants C_{11}, C_{12}, and C_{44} [27]. These elastic constants used in this work are obtained from first-principle calculations that have been performed by other studies in the literature . The relevant references are shown in the supplementary information.

$$\phi_{dil(m,c)} = \frac{(C_{11,m}-C_{12,m}-3C_{44,m})(2C_{11,c}+2C_{12,c})}{4C_{11,m}-4C_{12,m}+12C_{44,m}+5C_{11,c}+10C_{12,c}} \times \frac{(V_m-V_c)^2}{V_c} \qquad \text{(Eq. 4)}$$

Elastic constant datasets for the following calculations are obtained from [28], and the use of Eq. 4 permits the use of elastic constants from a single source, so that any errors in calculations are consistent and normalised for each composition, allowing comparison of results. The total strain in a multicomponent system may be considered as a function of the sum of the pairwise interactions of all of the alloying components. The equation can therefore be written as:

$$\phi_{dil} = \sum_{m,c=n}^{n=1,2,3\ldots} c_m\, c_c\, \phi_{dil(m,c)} \qquad \text{(Eq. 5)}$$

where $C_{11,m}$, $C_{12,m}$, and $C_{44,m}$ are the elastic constants of the matrix and $C_{11,c}$, $C_{12,c}$, and $C_{44,c}$ are the elastic constants of the centre.

3. Validation of parameters utilising a 212 composition dataset.

A dataset of 212 compositions consisting of a mixture of HEAs and CCAs (FCC, BCC, Sigma, Laves, B2, Mu, and a mixture of these) from the literature is used to validate the theoretical calculations presented here. The dataset list with its references is located in the supplementary information. Included are calculated value for the ROM primary quantum number, ROM VEC, enthalpy of mixing, dilatational strain, Φ_{dil} (Eq. 5), and elastic strain energy, Φ_{el} (Eq. 2).

Fig. 1 shows biplots of the Miedema enthalpy of mixing against the strain energies utilising both methods. The compositions are classified into groups according to phases that they exhibit, and their centres are determined by minimising the Euclidean distance between each group following the method used in [5]; the bounding radii are equivalent to the standard deviations of each group. The separation between the phases along the y-axis is more significantly spaced in Fig. 1 (b) compared to Fig. 1 (a). It is of note that whilst utilising ΔH_{el} values, the strain in a dilated matrix of a solid solution that leads to intermetallic phase stability is higher than the strain values for solid-solution (FCC & BCC) and mixed phases. Comparatively, whilst utilising ΔH_{dil} values (which consider the pairwise interaction as a function of the strain contributions from both matrix and inclusion) the bounding area for intermetallic compositions shows an increase in the range of ΔH_{dil} values. It is generally acknowledged that a chemical rearrangement (on diffusion/heating) leading to the nucleation/growth of a secondary phase generally leads to a reduction in the interfacial energy between these phases. When the intermetallic-forming alloying components are allowed to find their equilibrium positions with one another, they will possess highly negative ΔH_{mix} values (due to a preference for dissimilar bonding) and a reduction in mechanical strain (arising from the resulting chemical rearrangement). This is in good agreement with the idea of interfacial energy reduction.

The compositions are identified as either BCC, FCC, IM or MIXED. The IM designation means that they do not show any BCC or FCC structures, while the MIXED designation means that they were characterised having both the FCC/BCC phase and intermetallic phase.

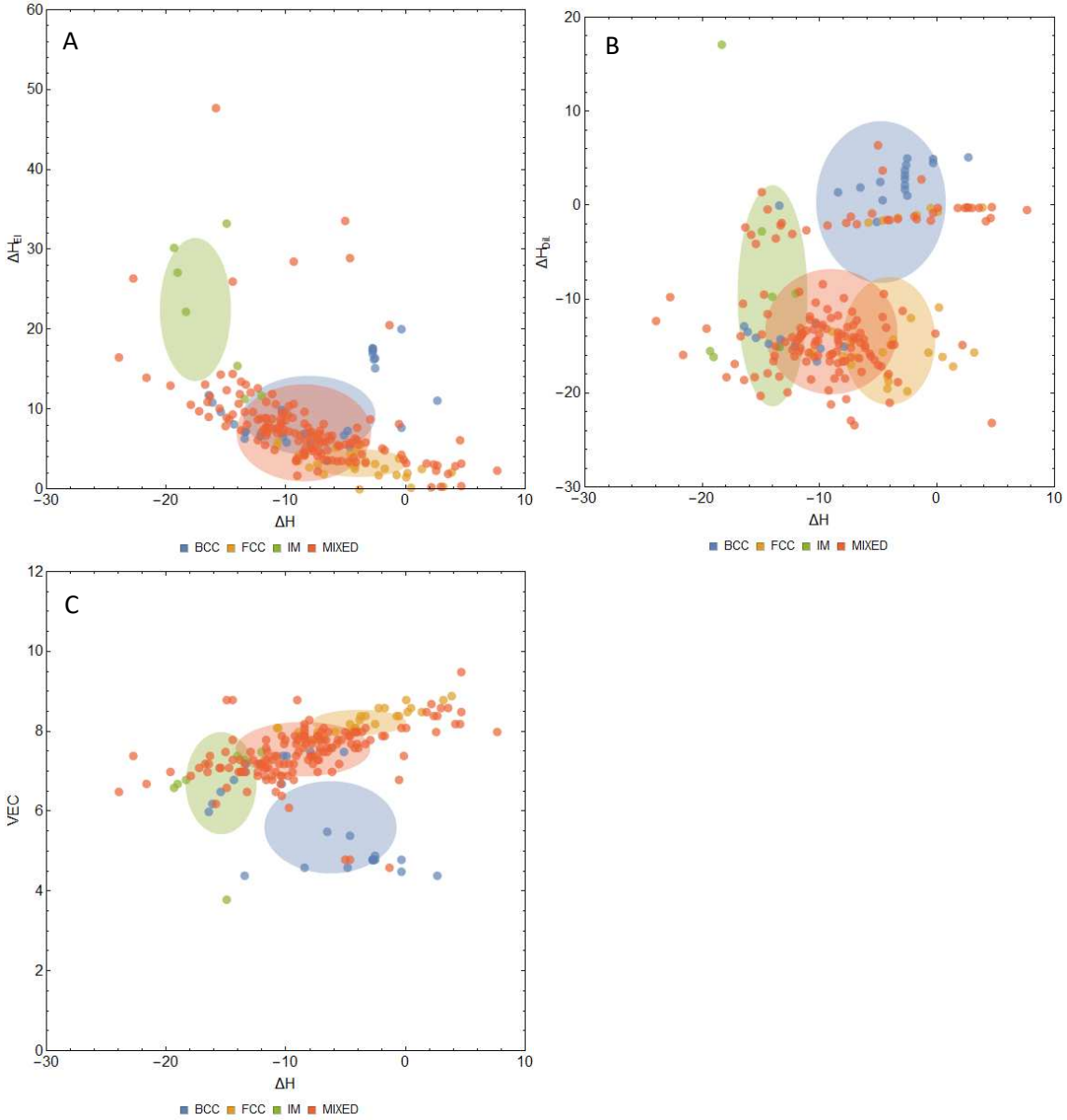

Figure 1. Meta-analysis of 212 MCA compositions utilising (a) ϕ_{el} [10,13] in a biplot with the enthalpy of mixing ΔH; (b) ϕ_{dil} as defined in Eq. 5 in a biplot with the Miedema enthalpy of mixing ΔH; and (c) the valence electron concentration, VEC for baseline comparison. For simplicity, the alloy database (cf. Supplementary information) has been classified into the four groups: BCC, FCC, intermetallic IM, and **MIXED** phases. Alloys in the BCC, FCC, and IM groups are included only when they display one identifiable phase from their XRD patterns. The encapsulating area for each group is determined by obtaining the radius and centre position of each group through minimising the Euclidean distance [5].

The relative locations of the areas encapsulating the BCC group in both figures are also observed to be rather different to one another. An investigation of the dataset shows that the compositions in the BCC group can be generally separated into Al-containing and Zr-containing compositions which tend to inhabit different areas of the biplot. Al-containing CCAs are generally alloyed with Ni and/or Co, and these together are known to stabilise the ordered BCC (B2) structure [29] – and it may be questionable therefore if Al-containing CCAs are truly of the BCC phase as it has been reported that the BCC B2 phases are generally coherently

present with/within each other. Considering just the Zr-containing compositions would shift the bounding circle for the ΔH_{el} biplot in Fig. 1 a to {0.4,15}, which would make the placements of the bounding regions comparable to the ΔH_{dil} biplot. The coordinates are shown in Table 1.

The use of either parameter appears to have its own merits, as both appear to be able to distinguish phase formation of the different alloy systems. The key difference between both parameters are their treatment of the intermetallic group, due to the overlap between the green IM bounding circle with the MIXED region.

Table 1. Cluster centre coordinates and Standard deviation values for the analysis in Fig. 1 and Fig. 2.

ΔH_{El} vs. ΔH	Grouped Phase Differentiation					Intermetallic Phase Differentation				
		Centre		Std. Dev.			Centre		Std. Dev.	
		x	y	x	y		x	y	x	y
	BCC	8.05	9.16	5.53	4.95	Laves	-15.2	12.67	6.17	5.68
	FCC	3.84	3.2	3.93	1.75	B2	-7.92	-6.77	2.54	0.73
	IM	-17.53	22.41	2.97	8.97	Sigma	-10.77	7.89	2.32	2.44
	MIXED	-8.54	7	5.63	6.09	Mu	-3.5	8.22	0.78	0.75

VEC vs. ΔH	Grouped Phase Differentiation					Intermetallic Phase Differentation				
		Centre		Std. Dev.			Centre		Std. Dev.	
		x	y	x	y		x	y	x	y
	BCC	-6.27	5.59	5.53	1.16	Laves	-15.82	7.89	6.17	0.86
	FCC	-3.92	8.21	3.93	0.32	B2	-7.8	7.4	2.54	0.34
	IM	-15.41	6.69	2.97	1.28	Sigma	-10.71	7.2	2.32	0.52
	MIXED	-8.55	7.56	5.63	0.68	Mu	-3.66	7.94	0.78	0.14

ΔH_{Strain} vs. ΔH	Grouped Phase Differentiation					Intermetallic Phase Differentation				
		Centre		Std. Dev.			Centre		Std. Dev.	
		x	y	x	y		x	y	x	y
	BCC	-4.78	0.29	5.53	8.61	Laves	-16.5	-10.42	6.17	4.72
	FCC	-4.09	-14.47	3.93	6.82	B2	-8.19	-13.58	2.54	8.65
	IM	-14	-9.68	2.97	11.78	Sigma	-10.79	-14.18	2.32	2.75
	MIXED	-9.02	-13.44	5.63	6.67	Mu	-3.18	-13.64	0.77	6.91

4. Intermetallic/complex phase differentiation

In the following section, the same methodology is applied to further distinguish the IM and MIXED phases. The alloys are classified to either the Laves, B2, Sigma, or Mu designations as long as they display the Laves, B2, Sigma, or Mu phase either singularly, or in combination with a solid solution phase (*i.e.* FCC/BCC). If an alloy displays two type of intermetallic phases, they are not included in the analysis.

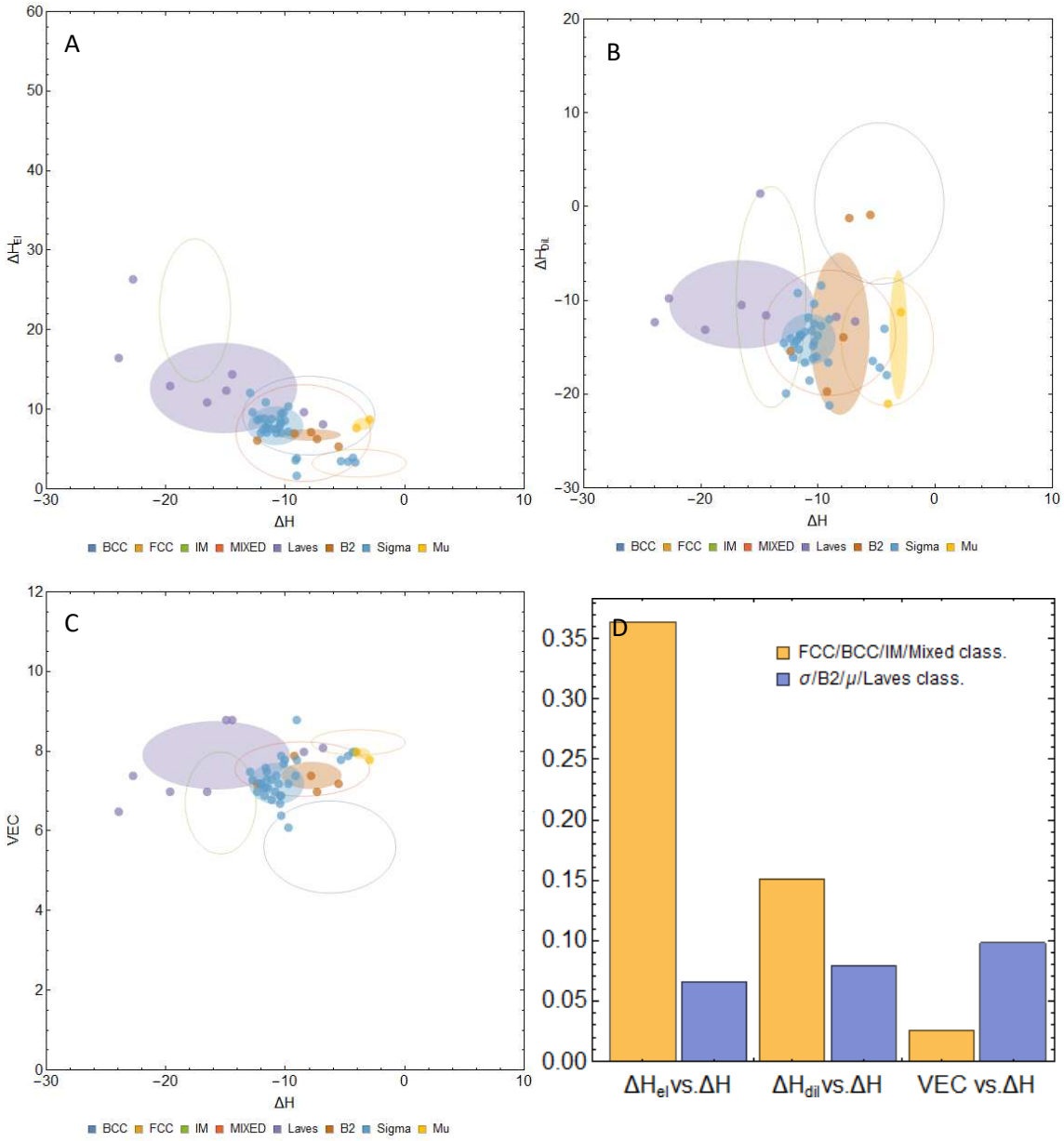

Figure 2. Meta-analysis of 212 MCA compositions utilising (a) ϕ_{el} [10,13] in a biplot with the enthalpy of mixing ΔH; (b) ϕ_{dil} as defined in Eq. 5 in a biplot with the Miedema enthalpy of mixing ΔH; (c) the valence electron concentration; and d) The overlap fraction, VEC for baseline comparison. The alloy database (*cf.* Supplementary information) has been reclassified to distinguish between four complex phases: Laves, B2, Sigma, and Mu.

Fig. 2 shows the results of the applied methodology. The original bounding circles are shown in the figure for comparison; the coordinates of the intermetallic bounding circles are displayed in Table 1. Some degree of overlap can be observed in these plots, although the different intermetallic phases are generally interspaced between the IM and MIXED clusters, as may be expected.

The degree of overlap between each phase evaluated in Figs. 1 and 2 was evaluated in Figs. 1 and 2 and is shown in Fig. 2 (d). The results show that the ΔH_{el} *vs.* ΔH plot shows the greatest overlap when differentiating between the grouped phases (*cf.* Fig. 1) and the lowest overlap between the intermetallic phases. In contrast, the ΔH_{el} *vs.* VEC plot shows the lowest overlap when distinguishing between the grouped phases and the largest overlap between

the intermetallic phases. The ΔH_{dil} *vs.* ΔH biplot on the other hand shows an intermediate degree of overlap when compared to either two biplots.

The results suggest that for alloy design, ΔH_{dil} *vs.* ΔH biplots may be better for general purpose use, with the other biplots used depending on the circumstance.

Acknowledgements

ZL would like to thank Dr. A. Quintana-Nedelcos for useful discussions on the work.

Funding Sources

This work was supported by the Leverhulme Trust Research grant Scheme [RPG-2018-324]. RG would like to acknowledge a Fellowship supported by the Royal Academy of Engineering under the RAEng/Leverhulme Trust Senior Research Fellowships scheme [LTSRF1718_14_39].

Contribution

Design of experiment: ZYL; Analysis: ZYL; Figures and writing: ZYL; Editing: NAM, RG; Supervision: NAM, RG

References

[1] B. Cantor, I.T.H. Chang, P. Knight, A.J.B. Vincent, Microstructural development in equiatomic multicomponent alloys, Materials Science and Engineering A, Phys. Rev. B Condens. Matter. 375–377 (2004) 213–218.

[2] J.W. Yeh, S.K. Chen, S.J. Lin, J.Y. Gan, T.S. Chin, T.T. Shun, C.H. Tsau, S.Y. Chang, Nanostructured high-entropy alloys with multiple principal elements: Novel alloy design concepts and outcomes, Adv. Eng. Mater. 6 (2004) 299–303.

[3] D.B. Miracle, O.N. Senkov, A critical review of high entropy alloys and related concepts, Acta Mater. 122 (2017) 448–511. https://doi.org/10.1016/j.actamat.2016.08.081.

[4] Z. Leong, J.S. Wróbel, S.L. Dudarev, R. Goodall, I. Todd, D. Nguyen-Manh, The Effect of Electronic Structure on the Phases Present in High Entropy Alloys, Sci. Rep. 7 (2017) 39803. https://doi.org/10.1038/srep39803.

[5] Z. Leong, Y. Huang, R. Goodall, I. Todd, Electronegativity and enthalpy of mixing biplots for High Entropy Alloy solid solution prediction, Mater. Chem. Phys. (2017). https://doi.org/10.1016/j.matchemphys.2017.09.001.

[6] S.A. Kube, J. Schroers, Metastability in high entropy alloys, Scr. Mater. 186 (2020) 392–400. https://doi.org/10.1016/j.scriptamat.2020.05.049.

[7] J. Cornide, M. Calvo-Dahlborg, S. Chambreland, L.A. Dominguez, Z. Leong, U. Dahlborg, A. Cunliffe, R. Goodall, I. Todd, Combined atom probe tomography and TEM investigations of CoCrFeNi, CoCrFeNi-Pdx (x=0.5, 1.0, 1.5) And CoCrFeNi-Sn, Acta Phys. Pol. A. 128 (2015).

[8] E.J. Pickering, R. Munoz-Moreno, H.J. Stone, N.G. Jones, Precipitation in the equiatomic high-entropy alloy CrMnFeCoNi, Scr. Mater. 113 (2016).

[9] F. Otto, A. Dlouhý, K.G. Pradeep, M. Kuběnová, D. Raabe, G. Eggeler, E.P. George, Decomposition of the single-phase high-entropy alloy CrMnFeCoNi after prolonged anneals at intermediate temperatures, Acta Mater. 112 (2016) 40–52. https://doi.org/10.1016/j.actamat.2016.04.005.

[10] A.F. Andreoli, J. Orava, P.K. Liaw, H. Weber, M.F. de Oliveira, K. Nielsch, I. Kaban, The elastic-strain energy criterion of phase formation for complex concentrated alloys, Materialia. 5 (2019) 100222. https://doi.org/10.1016/j.mtla.2019.100222.

[11] I. Toda-Caraballo, P.E.J. Rivera-Díaz-del-Castillo, A criterion for the formation of high entropy alloys based on lattice distortion, Intermetallics. 71 (2016) 76–87. https://doi.org/10.1016/j.intermet.2015.12.011.

[12] Y. Zhang, X. Yang, P.K. Liaw, Alloy design and properties optimisation of high-entropy alloys, J. Mater. Miner. Min. Soc. 64 (2012) 830–838.

[13] A.B. Melnick, V.K. Soolshenko, Thermodynamic design of high-entropy refractory alloys, J. Alloys Compd. 694 (2017) 223–227. https://doi.org/10.1016/j.jallcom.2016.09.189.

[14] M.G. Poletti, L. Battezzati, Electronic and thermodynamic criteria for the occurrence of high entropy alloys in metallic systems, Acta Mater. 75 (2014) 297–306. https://doi.org/10.1016/j.actamat.2014.04.033.

[15] L.A. Dominguez, R. Goodall, I. Todd, Prediction and validation of quaternary high entropy alloys using statistical approaches, Mater. Sci. Technol. 31 (2015) 1201–1206. https://doi.org/10.1179/1743284715Y.0000000019.

[16] Y.F. Ye, Y.H. Zhang, Q.F. He, Y. Zhuang, S. Wang, S.Q. Shi, A. Hu, J. Fan, Y. Yang, Atomic-scale distorted lattice in chemically disordered equimolar complex alloys, Acta Mater. 150 (2018) 182–194. https://doi.org/10.1016/j.actamat.2018.03.008.

[17] D.G. Pettifor, Theory of the Heats of Formation of Transition-Metal Alloys, Phys. Rev. Lett. 42 (1978) 846.

[18] S. Guo, N. C, L. J, L.C. T, Effect of valence electron concentration on stability of fcc or bcc phase in high entropy alloys, J. Appl. Phys. 109 (2011) 10.

[19] J.W. Christian, The theory of transformations in metals and alloys. Pt. 2: [...], 3. ed, Pergamon, Amsterdam, 2002.

[20] A.R. Miedema, The electronegativity parameter for transition metals: Heat of formation and charge transfer in alloys, J. Common Met. 32 (1973) 117–136. https://doi.org/10.1016/0022-5088(73)90078-7.
[21] S. Guo, C.T. Liu, Phase stability in high entropy alloys: Formation of solid-solution phase or amorphous phase, Prog. Nat. Sci. Mater. Int. 21 (2011) 433–446. https://doi.org/10.1016/S1002-0071(12)60080-X.
[22] A. Takeuchi, A. Inoue, Mixing enthalpy of liquid phase calculated by miedema's scheme and approximated with sub-regular solution model for assessing forming ability of amorphous and glassy alloys, Intermetallics. 18 (2010) 1779–1789. https://doi.org/10.1016/j.intermet.2010.06.003.
[23] A. Takeuchi, A. Inoue, Calculations of Mixing Enthalpy and Mismatch Entropy for Ternary Amorphous Alloys, Mater. Trans. JIM. 41 (2000) 1372–1378. https://doi.org/10.2320/matertrans1989.41.1372.
[24] J.D. Eshelby, The Continuum Theory of Lattice Defects, in: Solid State Phys., Elsevier, 1956: pp. 79–144. https://doi.org/10.1016/S0081-1947(08)60132-0.
[25] D. Kashchiev, Nucleation basic theory with applications, Butterworth Heinemann, Oxford; Boston, 2000. http://www.engineeringvillage.com/controller/servlet/OpenURL?genre=book&isbn=9780750646826 (accessed February 20, 2016).
[26] W. Voigt, Theoretische Studien über die Elastizitätsverhältnisse der Kristalle. Göttingen 1887. Abh. königl. Ges. d, Wiss Bd. 34 (1887).
[27] A new semi-empirical method based on a distorted tetragonal scheme for the structure prediction and alloy design of multiple-component alloys, University of Sheffield, 2017. http://etheses.whiterose.ac.uk/id/eprint/17022 (accessed February 1, 2018).
[28] S.L. Shang, A. Saengdeejing, Z.G. Mei, D.E. Kim, H. Zhang, S. Ganeshan, Y. Wang, Z.K. Liu, First-principles calculations of pure elements: Equations of state and elastic stiffness constants, Comput. Mater. Sci. 48 (2010) 813–826. https://doi.org/10.1016/j.commatsci.2010.03.041.
[29] Y. Ma, B. Jiang, C. Li, Q. Wang, C. Dong, P. Liaw, F. Xu, L. Sun, The BCC/B2 Morphologies in AlxNiCoFeCr High-Entropy Alloys, Metals. 7 (2017) 57. https://doi.org/10.3390/met7020057.